Eur. J. Mech. B - Fluids 19 (2000) 871–888

S0997-7546(00)01110-9/FLA

Wave-envelope steepening in the Blasius boundary-layer

Jonathan J. Healey [1]

Department of Mathematics, Keele University, Staffordshire ST5 5BG, UK

(Received 10 March 2000; revised 25 June 2000; accepted 8 August 2000)

Abstract – Previous experiments into the evolution of small amplitude disturbances to the Blasius boundary layer have shown that modulated waves become nonlinear at lower amplitudes than unmodulated waves. In this paper we propose a mechanism that may account for this behaviour. It involves a wave-envelope steepening scenario analogous to water-wave overturning and shock formation. Larger amplitude parts of a modulated wave travel at a different speed to lower amplitude parts, due to the proposed nonlinear mechanism, leading to an asymmetry between the steepness of decaying and growing sections. These effects occur in the higher order Ginzburg–Landau equation, so this may be a useful model for the process. Results from a windtunnel experiment, and a direct numerical simulation, will be presented and analysed for this effect. Both show a clear progressive asymmetry developing as the amplitude, and hence nonlinearity, are increased. Comparison between the experiment and simulation highlights key differences between two- and three-dimensional nonlinear evolutions. © 2000 Éditions scientifiques et médicales Elsevier SAS

1. Introduction

When a small enough controlled disturbance is introduced to a laminar boundary layer, there will be a local response close to the source of excitation, and further away, if the disturbance contains unstable frequency components, there will emerge a superposition of downstream propagating normal mode solutions. This paper is concerned with the initial nonlinear modifications to this linear normal mode behaviour (the disturbances considered here are small enough for any transient algebraic growth to have taken place, and then decayed, all within the linear regime, and for the ultimate exponential growth to be the dominant growth mechanism).

Gaster [1] first reported that in wind tunnel experiments on the Blasius boundary layer wavepackets produced by a point source become nonlinear at lower amplitudes than purely harmonic disturbances. Stewartson and Stuart [2] showed that a wavepacket in a parallel shear layer can be governed by a complex Ginzburg–Landau equation, but the nonlinearity in this equation is of the same form as that for an unmodulated wave governed by a Landau equation. Eckhaus [3,4] has shown how the presence of modulation can destabilize an otherwise stable saturated nonlinear solution to the Landau equation, and in Eckhaus and Iooss [5] it is shown that this effect is particularly important in the Blasius boundary layer due to the smallness of the real part of the cubic coefficient in the Landau equation for this flow close to the critical Reynolds number. Natural laminar-turbulent transition, in a low freestream turbulence environment, is initiated by the linear evolution of randomly modulated waves, so an understanding of the effects of modulation will be important for a more complete description of natural transition.

Shaikh and Gaster [6], Shaikh [7,8] and Medeiros and Gaster [9,10] all present detailed experimental observations of the nonlinear evolution of modulated waves, both wavepackets and randomly modulated waves, the latter to simulate natural transition. However, no plausible model has yet been produced to account for, or

[1] E-mail: j.j.healey@keele.ac.uk

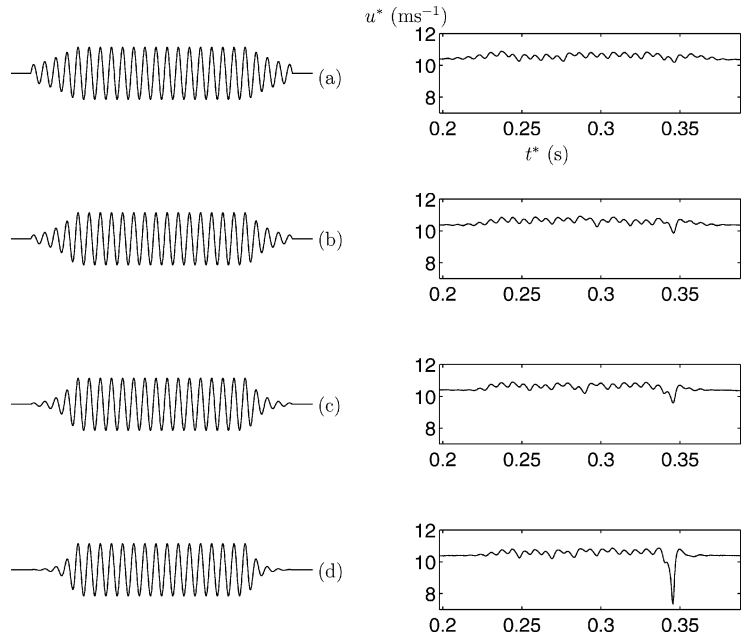

Figure 1. The left-hand column shows a set of modulated driving signals that were used to excite the boundary layer. The right-hand column shows the corresponding hot-wire signals (ensemble averaged) measured at a point one displacement thickness from the wall, and where $R_{\delta*} = 1980$, where $R_{\delta*}$ is the Reynolds number based on displacement thickness, u^* is the dimensional horizontal component of velocity, t^* is the dimensional time, and the freestream velocity was 18 ms^{-1}.

explain the observed behaviour. Healey [11] used a different kind of modulated disturbance, which contained a growing section and a decaying section separated from one another by an unmodulated section. This allowed the behaviour of growing and decaying modulation to be investigated in isolation. The strength of modulation was then systematically adjusted. *Figure 1* is taken from Healey [11] and summarizes the main finding of that paper (it is presented here for convenience, and motivates the present work). What is striking is that as the strength of modulation increases, a violent nonlinear breakdown to a spike is produced at the decaying part of the signal, but a similarly strong growing part of modulation produces no such effect.

It is well known that turbulent spots evolving from linear wavepackets show a strong asymmetry between the front and back, see Amini and Lespinard [12], and spikes tend to form at the back of turbulent spots, e.g. Klingmann [13]. Here we investigate the origins of this asymmetry, and show that asymmetry occurs during the early, weakly nonlinear, stages that precede spike formation.

In section 2 a model is proposed (a higher order Ginzburg–Landau equation) that might explain this asymmetry between growing and decaying modulation. The model applies only to the initial weakly nonlinear stages before the spike occurs and is not intended to describe the spike itself. It describes the evolution of the amplitude envelope and it contains terms which cause an asymmetric steepening of the envelope. In section 3, we present new experimental results and analyse this data for signs of wave-envelope steepening, which is indeed found to occur. In a long randomly modulated wavy disturbance, it is interesting to note that it is precisely those places in the data showing the strongest steepening effects that are where spikes are first seen. The experiments involve three-dimensional waves, but the model predicts that even two-dimensional waves can show steepening effects. A direct numerical simulation of two-dimensional modulated waves has been carried out and the results, which again show steepening effects, are presented in section 4. The amplitude is found to increase close to where the steepening is occuring, and this may explain why modulation can make disturbances

more likely to undergo a nonlinear breakdown. The differences between two- and three-dimensional evolution are examined further in section 5, with additional data analysis showing evidence for subharmonic resonance concentrated in regions of envelope-steepening. Conclusions and discussion are given in section 6.

2. Model producing asymmetric modulation

When a disturbance has a small amplitude that is changing slowly compared with the wavelength or frequency of the disturbance (depending on whether a spatial, temporal or spatio-temporal analysis is being undertaken) then a weakly nonlinear theory is possible and nonlinear amplitude equations can be derived using multiple-scales theory. Different types of equations are obtained depending on the disturbances being considered. If the disturbance is periodic in either space or time, then the disturbance amplitude A will typically satisfy a Landau equation of the form

$$\frac{\mathrm{d}A}{\mathrm{d}X} = aA + lA|A|^2, \tag{1}$$

where X is the length scale over which the amplitude changes. This was first shown by Stuart [14] for channel flow and Watson [15] produced the spatial version (1). The constant l is called the Landau coefficient and the sign of its real part determines whether nonlinearity acts to enhance or moderate disturbance growth. The real part of a gives the growth rate of linear stability theory and its imaginary part corresponds to the small change in wavelength of the wave compared to that of the neutral wave about which the expansion has been taken.

Before considering modulated waves, we draw attention to an additional difficulty in deriving amplitude equations for boundary layers. In linear stability theory, transform methods can be used to reduce the disturbance equations to ordinary differential equations, provided that the wavelength is short compared to distances over which the boundary layer is growing. This turns out to be a reasonable approximation for two-dimensional waves in the Blasius boundary layer, see Fasel and Konzelmann [16], Bertolotti et al. [17] and Klingmann et al. [18]. However, for (1) to apply, the boundary layer must also have an approximately constant thickness over the longer X scale. Sufficiently close to the neutral curve this will not be the case, since X can be made arbitrarily large by considering almost neutral waves. These nonparallel effects can be included in the weakly nonlinear analysis in the large Reynolds number limit, and Ruban [19] and Hall and Smith [20] show that this leads to an amplitude equation where the coefficient a in (1) is replaced by a term proportional to X, reflecting the change in linear growth rate experienced by a wave as it propagates downstream. Smith [21,22] used the large Reynolds number triple-decked structure of the disturbances near the lower branch of the neutral curve to show that near the lower branch the Landau coefficient has negative real part.

Separate asymptotic theories are required near the upper and lower branches, and yet, as discussed below, a nonlinear theory for modulated waves must be based on the critical Reynolds number where linear disturbances share characteristics of both the upper and lower branches. However, Hultgren [23] showed that the critical Reynolds number and upper branch can be obtained if a certain higher order term is included in the lower branch asymptotic theory. Healey [24] has now extended the lower branch theory by going to a high enough order in the expansion using a symbolic manipulation package, so that both the upper branch and nonparallel effects are included consistently. This can provide a basis for deriving a nonparallel theory for modulated waves.

The presence of pressure gradients can significantly alter the nature of the instability, e.g. converting a viscous instability to an inviscid instability, which changes the upper branch asymptotic theory but not the lower branch theory. Healey [25] has found that, as in Healey [26], disturbances closely resemble the triple-decked lower branch asymptotic structures at the Reynolds numbers for transition in wind tunnels, and so the extended lower branch theory for calculating the critical Reynolds number will also be useful for more general boundary layers.

An amplitude equation for modulated waves can only be used when the modulation is relatively weak, or else the separation between the scales of the oscillation and those of the envelope will not be possible. Weak modulation implies that only a narrow band of frequencies can be excited, and hence disturbances should be relatively close to the critical Reynolds number so that there is only a narrow frequency band of unstable waves. The starting point for the nonlinear theory of modulated waves is the linear wavepacket, which takes the form

$$A = \frac{A_0}{t^{1/2}} \exp\left(at - \frac{(x - c_g t)^2}{4bt} \right), \tag{2}$$

where x is streamwise distance, c_g is the group velocity of the wavepacket (which is the group velocity of the most unstable wave and is real), t is time and a and b are constants, see Benjamin [27]. This gives the familiar Guassian envelope for the wavepacket, which grows exponentially if the real part of a is positive, and shows that its spatial extent grows as the square-root of time. Stewartson and Stuart [2] exploited this structure by taking

$$T = \varepsilon t, \qquad \xi = \varepsilon^{1/2}(x - c_g t) \tag{3}$$

as the slow time and length scales for the evolution of the amplitude, where ε is a small parameter, and by considering an expansion around the critical Reynolds number for instability derived the complex Ginzburg–Landau equation for channel flow

$$\frac{\partial A}{\partial T} - b\frac{\partial^2 A}{\partial \xi^2} = aA + lA|A|^2. \tag{4}$$

There is a difficulty in choosing initial conditions for (4). At early enough times the $t^{1/2}$ term in (2) will dominate, and the nonlinear term will no longer be balanced with the other terms in (4). Stewartson and Stuart [2] proposed using initial conditions at small finite times and small finite initial amplitude A_0 to get around this problem. However, Jennings et al. [28], have shown that the evolution from a truely linear regime into one in which nonlinearity starts to become important can be studied if A_0 is taken as a small parameter. It is then necessary to wait for a relatively long time $T \gg 1$ before the amplitude is large enough for nonlinear effects to become important, by which time significant spreading of the wavepacket will have occured, thereby weakening the diffusive term with coefficient b. They show that this can have important consequences for the existence and nature of singularities in (4) when the real part of l is positive.

Modulational effects appear via the diffusive term in (4), which is linear. The nonlinear term is the same for both (1) and (4). Therefore, this theory does not account for the tendency for modulated waves to become nonlinear at lower amplitudes, nor does it produce an asymmetry between growing and decaying sections of modulation. Both of these features have been observed in experiments, e.g. in *figure 1*. Nonetheless, the diffusive term can produce destabilizing effects that tend to enhance modulation, despite the fact that in the linear version of the equation, the role of this term is to smooth out and reduce modulation. This process was first discussed by Eckhaus [3,4] and it is instructive to see how this comes about. Substituting $A = R\mathrm{e}^{i\theta}$, where R and θ are real, into (4) and equating real and imaginary parts leads to

$$\frac{\partial R}{\partial T} = a_r R + l_r R^3 + b_r \left[\frac{\partial^2 R}{\partial \xi^2} - R\left(\frac{\partial \theta}{\partial \xi} \right)^2 \right] - b_i \left[2\left(\frac{\partial R}{\partial \xi} \right)\left(\frac{\partial \theta}{\partial \xi} \right) + R\frac{\partial^2 \theta}{\partial \xi^2} \right], \tag{5}$$

$$R\frac{\partial \theta}{\partial T} = a_i R + l_i R^3 + b_i \left[\frac{\partial^2 R}{\partial \xi^2} - R\left(\frac{\partial \theta}{\partial \xi} \right)^2 \right] + b_r \left[2\left(\frac{\partial R}{\partial \xi} \right)\left(\frac{\partial \theta}{\partial \xi} \right) + R\frac{\partial^2 \theta}{\partial \xi^2} \right], \tag{6}$$

where the subscripts r and i denote real and imaginary parts respectively. There is a family of constant amplitude solutions to (5) and (6), parameterized by the constants α_0 and θ_0, given by

$$R = R_0, \tag{7}$$

$$\theta = \theta_0 + \alpha_0 \xi + (a_i + l_i R_0^2 - b_i \alpha_0^2) T, \tag{8}$$

where

$$R_0 = \left(\frac{b_r \alpha_0^2 - a_r}{l_r} \right)^{1/2} \tag{9}$$

and $l_r \neq 0$. Note that $\alpha_0 = 0$ corresponds to the unmodulated equilibrium solution of the Landau equation and θ_0 gives trivial translations in the ξ and T coordinates.

The linear stability of this solution can be examined by adding small perturbations to (7) and (8) to give

$$R = R_0 + \varepsilon_1 R_1 \mathrm{e}^{i\alpha\xi + \sigma T}, \tag{10}$$

$$\theta = \theta_0 + \alpha_0 \xi + (a_i + l_i R_0^2 - b_i \alpha_0^2) T + \varepsilon_1 \theta_1 \mathrm{e}^{i\alpha\xi + \sigma T}, \tag{11}$$

where R_1 and θ_1 are constants, and the condition for instability is $\mathrm{Re}(\sigma) > 0$. Substituting these expressions into (5) and (6), and linearizing in ε_1, gives

$$\sigma R_1 = -2a_r R_1 - b_r (\alpha^2 R_1 + 2i\alpha\alpha_0 R_0 \theta_1 - 2\alpha_0^2 R_1) + b_i (\alpha^2 R_0 \theta_1 - 2i\alpha\alpha_0 R_1), \tag{12}$$

$$\sigma R_0 \theta_1 = 2l_i R_0^2 R_1 - b_i (\alpha^2 R_1 + 2i\alpha\alpha_0 R_0 \theta_1) - b_r (\alpha^2 R_0 \theta_1 - 2i\alpha\alpha_0 R_1). \tag{13}$$

Eliminating R_1 and θ_1 from (12) and (13) gives a quadratic equation for σ. When $\alpha_0 = 0$ and α is small the solutions are

$$\sigma = -\left(b_r + \frac{b_i l_i}{l_r} \right) \alpha^2 + \mathrm{O}(\alpha^4), \tag{14}$$

$$\sigma = -2a_r + \mathrm{O}(\alpha^2). \tag{15}$$

Taking $\alpha = 0$ in (15) gives the stability of the solution in the absence of any modulation. Modulational instability is predicted by (14) when

$$b_r + \frac{b_i l_i}{l_r} < 0. \tag{16}$$

At the critical Reynolds number $b_r > 0$, so this instability of the unmodulated equilibrium solution depends on the existence of nonzero b_i and l_i. However, when $\alpha_0 \neq 0$, instability is possible even if $l_i = b_i = 0$. In this case the solution (14) is replaced by

$$\sigma = -\frac{b_r (a_r - 3\alpha_0^2 b_r)}{a_r - \alpha_0^2 b_r} \alpha^2 + \mathrm{O}(\alpha^4) \tag{17}$$

giving instability for

$$\frac{a_r}{3b_r} < \alpha_0^2 < \frac{a_r}{b_r} \tag{18}$$

when $a_r > 0$. Further cases have been studied by Stuart and DiPrima [29] who also showed that this modulational instability is equivalent to the Benjamin–Feir instability proposed in Benjamin and Feir [30] for water waves. Although this gives a mechanism that can cause waves to become more modulated, it does not produce asymmetry between growing and decaying sections.

However, (4) only represents the leading order equation for modulated waves. At next order in the expansion Ikeda [31] found that the equation takes the form

$$\frac{\partial A}{\partial T} - b \frac{\partial^2 A}{\partial \xi^2} = aA + lA|A|^2 + \varepsilon^{1/2} m |A|^2 \frac{\partial A}{\partial \xi} + \varepsilon^{1/2} n A^2 \frac{\partial \bar{A}}{\partial \xi}. \tag{19}$$

Weinstein [32] derived higher order corrections to (4) using multiple scales theory and found additional terms proportional to $\varepsilon^{1/2}\partial^3 A/\partial\xi^3$ and $\varepsilon A|A|^4$. Johnson [33] derived the equivalent equation for water waves in the case where the cubic coefficient is zero and found that the nonlinear spatial gradient terms and the quintic term all appear at leading order (an additional nonlinear term involving an integral with respect to ξ and derivative with respect to T was also found, but no third derivative in ξ). Dysthe [34] calculated higher order terms for the water wave problem when the cubic coefficient is not small and obtained the nonlinear spatial gradient terms and a third spatial derivative like Weinstein, and also that the quintic term was absent. Dysthe's analysis was for waves modulated in two spatial directions; the derivatives in the direction perpendicular to the propagation direction are linear. The main difference between the water wave problem and that for waves in a viscous shear layer is that the former is conservative, leading to coefficients that are either real or purely imaginary.

Of key importance here are the nonlinear spatial gradient terms in (19). Ikeda [31] showed with numerical simulations that these terms lead to an asymmetry about the centre of the wavepacket. The origin of this behaviour can be seen by substituting $A = R\mathrm{e}^{i\theta}$ into (19), then equating the real parts gives

$$\frac{\partial R}{\partial T} + C\frac{\partial R}{\partial \xi} - b_r\frac{\partial^2 R}{\partial \xi^2} = DR + LR^3, \tag{20}$$

where

$$C = -\varepsilon^{1/2}(m_r + n_r)R^2 - 2b_i\frac{\partial\theta}{\partial\xi}, \tag{21}$$

$$D = a_r + b_i\frac{\partial^2\theta}{\partial\xi^2} + b_r\left(\frac{\partial\theta}{\partial\xi}\right)^2, \tag{22}$$

$$L = l_r - \varepsilon^{1/2}(m_i + n_i)\frac{\partial\theta}{\partial\xi}. \tag{23}$$

The first-order spatial derivative on the left-hand side of (20) represents a convective term and means that the wavepacket propagates at a speed C relative to the linear group velocity. Equation (21) shows that the propagation velocity depends on the square of the amplitude of the envelope. Whether the speed increases or decreases with amplitude depends on the sign of the term $m_r + n_r$. An amplitude dependent velocity is the key ingredient for asymmetric envelope steepening behaviour analgous to water-wave over-turning or shock formation.

Note that although in general the envelope steepening terms are a small correction to the leading order wavepacket evolution, they do capture a qualitatively different type of behaviour to that found at leading order. Sen and Vashist [35] used a parallel flow theory to calculate l for Blasius flow, and found that l_r changes sign near the critical Reynolds number. The same result was found in direct numerical simulations for the full nonparallel problem by Houten et al. [36,37]. It is apparent from (14) that if l_r is small then the modulational instability can be very strong, and this case has been studied by Eckhaus and Iooss [5] in the context of Blasius flow.

If both l_r and l_i change sign near the critical Reynolds number then steepening effects will be a leading order effect, as in Johnson [33]. Estimates of l presented in Moresco and Healey [38] show that $l_i < 0$ all around the neutral curve for Blasius flow, but that including thermal effects in both the basic flow and the stability equations can significantly change l, allowing multiple changes in sign of l_r and l_i to occur with potentially important consequences for the amplitude equation for modulated waves.

Li et al. [39] have developed a theory for the development of the spike itself, which also involves a gradient steepening process. However, their theory is for the steepening of the wave rather than for the wave-envelope, and would apply at a later stage in the evolution of the disturbance than is being considered here.

In the next section we examine new experimental data to see whether this steepening effect can be detected, and whether it might play a role in the asymmetric behaviour seen in *figure 1*.

3. Experiments showing asymmetric modulation

We follow Shaikh and Gaster [6] and Shaikh [7,8] in investigating controlled randomly modulated disturbances as a model for natural transition induced by low amplitude background turbulence. However, while they followed the downstream evolution of disturbances, we have chosen to study the state of the disturbances at a fixed streamwise position and investigate how this changes as a function of forcing amplitude. In this way we can distinguish between those effects due solely to nonlinearity and those due to waves propagating linearly through a dispersive unstable medium. Also, while those authors focused attention on the development of the spike, which is a strongly three-dimensional phenomenon requiring many measurements across the span of the flow, we shall rely on measurements at a single spanwise station since we are interested in the early, weakly nonlinear, stages of the evolution. This may be justified as follows.

Weakly nonlinear theory describes a perturbation of linear behaviour. At Reynolds numbers of interest in transition experiments the strongest growing linear waves are two-dimensional, and even a point source will produce disturbances that are relatively weakly modulated in the spanwise direction, see Gaster and Grant [40], due to dispersive effects. As nonlinearity increases, the most noticable deviation from linear behaviour that they observed was growth of a pair of oblique waves; stronger three-dimensional effects occur later during the breakdown to turbulence. Given the relatively narrow band of spanwise wavenumbers excited during these early stages, and high degree of spanwise coherence, it is plausible to assume that a single spanwise measurement can be representative of the wavepacket (a similar assumption was made in Gaster [41]). However, see the direct numerical simulation presented in section 4 for a discussion of purely two-dimensional behaviour, and the differences with the three-dimensional experiment.

A computer-generated pseudo-random driving signal was sent to a loudspeaker embedded in a flat plate aligned with a uniform flow in the low-turblence windtunnel that was situated in the Engineering Department at Cambridge University, Cambridge, UK (now located at Queen Mary and Westfield College, University of London). This acted as a point source of disturbances to a Blasius boundary layer. The signal consisted of a set of uniformly distributed numbers and had a white noise spectrum. The experimental set-up was the same as described in Healey [11], and measurements were taken one displacement thickness from the wall, a metre from the leading edge of the plate and with a freestream velocity of 20 ms^{-1} (kinematic viscosity for air under atmospheric conditions is approximately 1.4×10^{-5} m^2s^{-1}, giving a Reynolds number based on displacement thickness of order 2050). A set of measurements taken across the wall-normal direction is shown in *figure 12* of Healey [11] and shows that a spike looks broadly similar across most of the boundary layer. We assume that any robust feature present during the early stages of nonlinear development will also not be located in any narrow regions. One place where a narrow layer might be expected to produce local nonlinear behaviour is the critical layer, but this lies within the viscous wall layer at transitional Reynolds numbers, see Healey [26], and in this layer the disturbance amplitude drops to zero. Therefore, we assume that measurements at a single wall-normal position will be representative.

The sample frequency was 10000 Hz, which is about 30 times higher than the highest frequency unstable wave at this Reynolds number, giving well resolved waveforms. The sampling was phase-linked to the digital

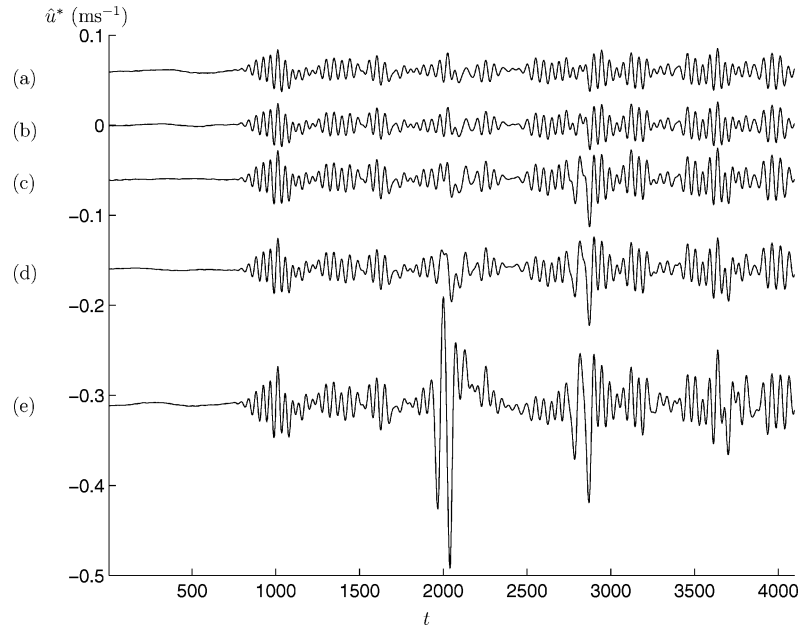

Figure 2. Hot-wire time series data (ensemble averaged) produced by forcing amplitudes of (a) 0.45, (b) 0.5, (c) 0.55, (d) 0.6, (e) 0.65, all in arbitrary units, and on the same vertical scale but with vertical offsets included to aid comparison. $\hat{u}^*$ is the dimensional horizontal component of the disturbance velocity and t is the time variable in arbitrary units.

to analogue converter that was used to drive the loudspeaker with the computer generated forcing signal, thus allowing ensemble averaging of repeated experiments to be used to improve the signal to noise ratio. The time scales used in the figures below correspond to units of sample period, e.g. the first 10000 records correspond to a time duration of 1 s. The amplitude of the signal sent to the digital to analogue converter was scaled so as to lie between 0 and 1 and amplitudes quoted below are based on these units (0 corresponds to no introduced disturbances, 1 gave highly irregular 'turbulent' behaviour).

At the lowest amplitudes of forcing there are no spikes in the time series data for the horizontal component of the disturbance velocity and the data takes the form of a randomly modulated envelope with a carrier wave whose frequency corresponds approximately to the most amplified wave according to linear stability theory. When the forcing amplitude is increased, a few isolated spikes appear in the time series. *Figure 2* focuses on a section of time series data where a spike is starting to form as the forcing amplitude increases. Comparing *figure 2*(*a*) with *figure 2*(*b*) shows the degree of reproducibility that was obtained in this experiment. At larger amplitudes than shown here a spike occurs first near record 2000 (this will be shown below in section 5 for a forcing of 0.7). We will be primarily concerned with the weakly nonlinear behaviour at forcing amplitudes up to 0.6, i.e. up to *figure 2*(*d*), before the strong nonlinear breakdown occurs.

One question posed by *figure 2* is why the disturbance near record 2000 should be the most susceptible to a strong nonlinear breakdown, when other parts, like near records 1000, 2800 and 3600, all have larger amplitudes. In fact, one distinguishing feature of the disturbance state around record 2000, is that there is already an asymmetric steepening of the envelope in this vicinity. *Figure 3*(*a*) shows the disturbance and its fitted envelope, around record 2000, at a smaller amplitude of forcing than any of the data shown in *figure 2*. Note that the decomposition of the disturbance into an oscillation plus envelope is not perfect, and the envelope, while broadly following the rise and fall of the intensity of the disturbance, also contains an oscillation with period close to that of the carrier wave. This relatively high frequency component to the envelope shows up

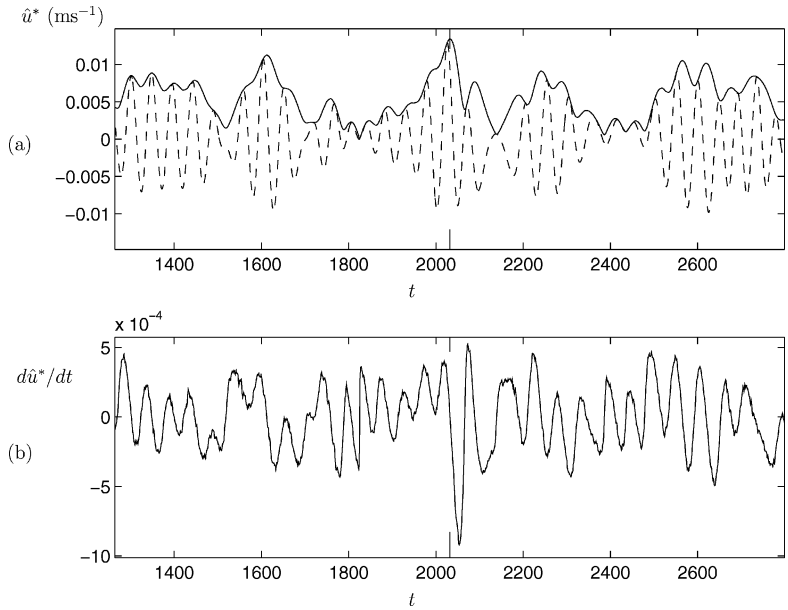

Figure 3. Behaviour for a forcing amplitude of 0.3 close to record 2000 where spikes form at larger forcing amplitudes. The vertical bars indicate the place in the time series where a spike first appears at larger forcing amplitudes. (a) Dashed line is the measured horizontal component of disturbance velocity, solid line is the envelope function calculated for this data. (b) The gradient of the envelope function (calculated using finite differences).

most strongly in the graph of the gradient of the envelope shown in *figure 3*(*b*). It is the trend underlying this oscillation that we are interested in. There is a strong asymmetry near record 2000, and it is remarkable that this region of strong decaying envelope corresponds so closely to where the spike will ultimately occur. If this is true in general, then it suggests that asymmetric envelope steepening may be an early precursor to strongly nonlinear spike formation embedded within the weakly nonlinear regime. This offers hope that the early stages of spike formation could be modelled, and hence, perhaps, that the location and onset of spikes could be predicted.

A more robust statistical measure of asymmetric envelope steepening is required, in addition to the local analysis of particular breakdown events. The model (20), together with (21), suggests that asymmetric steepening effects should tend to zero as the amplitude, R, tends to zero (i.e. as the linear regime is approached), and that it increases as the square of the amplitude. One way to characterize the strength of the asymmetric steepening effect, is to calculate the third moment of the gradient of the envelope. Let g_i be the gradient of the envelope at the ith point in a time series, then the asymmetry between the magnitude of growing and decaying sections, or skewness, σ, will be given by

$$\sigma^3 = \frac{1}{N}\sum_{i=1}^{N}\left(g_i - \bar{g_i}\right)^3, \tag{24}$$

where

$$\bar{g_i} = \frac{1}{N}\sum_{i=1}^{N} g_i \tag{25}$$

is the mean of the derivatives, and N is the number of data points in the time series.

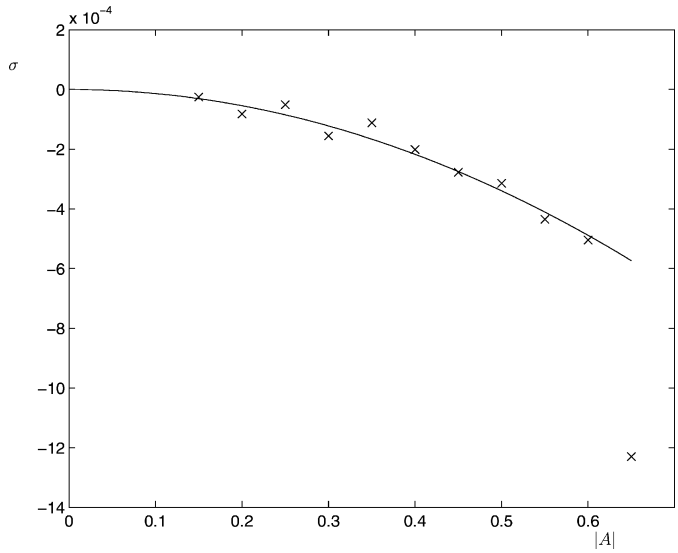

Figure 4. Crosses show the skewness of the derivatives, defined by (24), calculated at forcing amplitudes $|A|$. Solid curve is $\sigma = -13.6 \times 10^{-4}|A|^2$.

Figure 4 shows how σ varies over a range of forcing amplitudes. There is a clear, approximately quadratic, trend where the skewness becomes progressively more negative, indicating that decaying sections systematically steepen compared to growing sections as the amplitude increases. This indicates that larger amplitude parts are travelling more slowly than smaller amplitude parts (*figure 3*(*a*) shows a time series, the corresponding space series, i.e. graph of amplitude against downstream distance at a fixed time, would be reflected about a vertical axis, implying that positive spatial gradients are increasing). If (20) is a good model for this process, then this suggests that the term $m_r + n_r > 0$ so that the propagation velocity C decreases with amplitude R.

4. Direct numerical simulation showing asymmetric modulation

The direct numerical simulation of nonlinear two-dimensional waves in the Blasius boundary layer at Reynolds numbers relevant to the experiments can be carried out on a modern personal computer, provided that the disturbance amplitude is not too large. The code we have used is based on the velocity–vorticity formulation of the Navier–Stokes equations used by Davies and Carpenter [42], but extended for fully nonlinear simulations. It uses a Chebyshev pseudo-spectral method in the wall-normal direction, fourth order finite differences in the streamwise direction and second-order finite differences in time. The results presented here have been extracted from a broader numerical investigation into the role of amplitude equations for modulated and unmodulated disturbances to the Blasius boundary layer at finite Reynolds numbers, which will be published separately. Full details and results of this numerical study, including code validation, will appear in Houten et al. [36].

Figure 5(*a*) shows a time series (and its envelope) of the horizontal velocity component of a modulated two-dimensional disturbance. The driving signal was qualitatively similar to that shown in *figure 1* and the gradients of its growing and decaying sections had equal magnitude. The gradient of the disturbance envelope is shown in *figure 5*(*b*), and shows a clear asymmetry between the steepness of the growing section and that of the decaying section. *Figure 5*(*c*) shows the gradient of the time series itself. Note that there is no significant asymmetry in *figure 5*(*c*), demonstrating that the steepening effect is a property of the envelope and not the waveform itself, and so is suitable for modelling with amplitude equations.

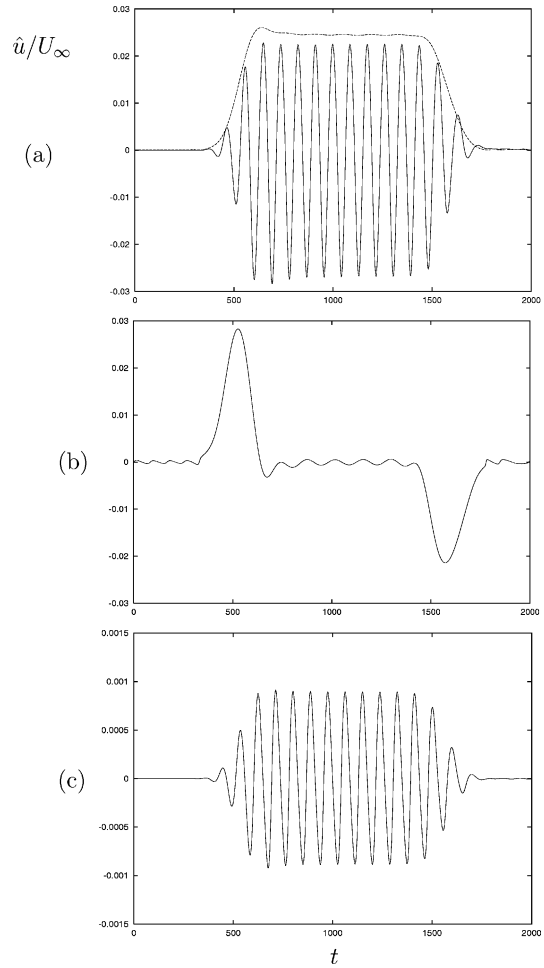

Figure 5. Direct numerical simulation of a two-dimensional modulated disturbance measured at the inner maximum of the disturbance amplitude in the wall-normal direction at a Reynolds number based on displacement thickness of 2187. (a) Solid line is the horizontal velocity component of the disturbance, dashed line is its envelope. (b) Gradient of the envelope shown in (a). (c) Gradient of the time series shown in (a).

In the two-dimensional simulation it is growing sections that are steeper, suggesting that $m_r + n_r < 0$, whereas the experiment showed that decaying sections steepen. It may be that the two-dimensional waves have $m_r + n_r < 0$, while three-dimensional waves have $m_r + n_r > 0$, and that in the experiment it is these latter waves that have the dominant effect. Note also that the envelope shown in *figure* $5(a)$ has a distinct maximum at the top of the growing section. This could be consistent with a focusing of energy in this region as larger amplitude parts catch up and coalesce with smaller amplitude parts.

In the next section we analyse the experimental results in more detail to see what evidence there is for three-dimensional behaviour in the regions of strongest envelope steepening.

5. Three-dimensional effects in the experiment

The experiments of Gaster and Grant [40] and Medeiros and Gaster [10] both show that oblique waves are excited at the onset of nonlinear behaviour. These waves have approximately half the frequency of the

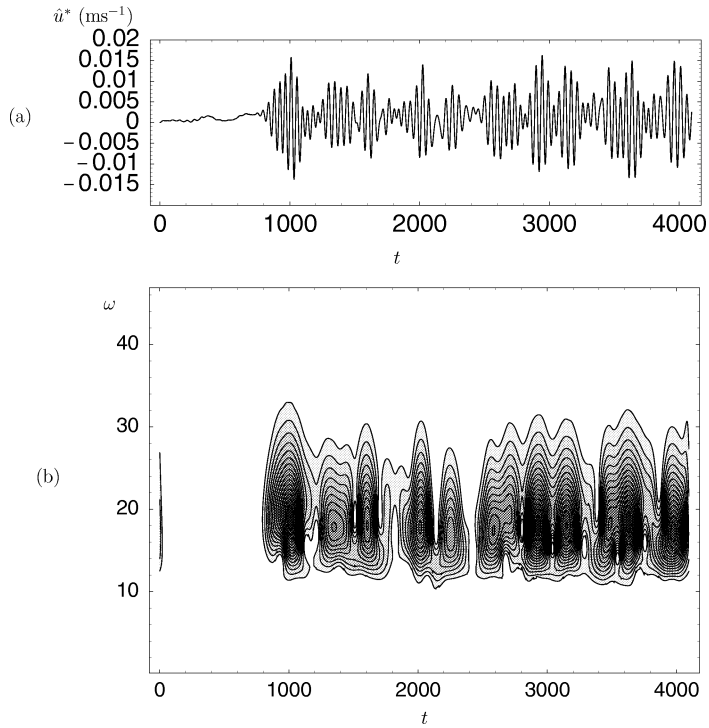

Figure 6. (a) shows the first 4096 records of the time series measured for a forcing of amplitude 0.3, $\hat{u}^*$ is the dimensional horizontal component of the disturbance velocity and t is the time variable in arbitrary units. (b) is the wavelet transform plane showing contours of constant $|W|$ defined by (27) with the darkest shadings representing the largest $|W|$. The frequency ω is related to a dimensionless frequency ω_δ based on displacement thickness by $\omega_\delta \approx 0.00540\omega$. The contours near $t = 0$ in (b) are spurious and are produced by using Fourier transforms to evaluate the convolution (27), which assumes periodic behaviour, identifying record 0 with record 4096.

most unstable waves and their spanwise wavenumber is similar to that predicted by Craik's [43] resonant triad interaction. We wish to investigate these subharmonic waves in regions where steepening is taking place.

Wavelet transforms provide a means of estimating the frequency content of a signal in local regions. The complex Morlet wavelet has been used, which consists of a Guassian envelope modulating a sinusoidal carrier wave:

$$w(t;\omega) = \mathrm{e}^{-(\omega t)^2/2 - im\omega t}, \tag{26}$$

where ω is the particular (local) frequency under consideration and m is an integer giving the approximate number of oscillations contained within the main part of the envelope. We have taken $m = 5$. For a fixed ω, the wavelet is translated to a time t_0 and projected onto the data $f(t)$ to give a wavelet coefficient

$$W(t_0,\omega) = \omega \int_{-\infty}^{\infty} f(t) w(t - t_0;\omega)\,\mathrm{d}t. \tag{27}$$

The normalization factor ω has been included so that wavelets of different frequencies will give wavelet coefficients of the same amplitude when applied to waves with different frequencies but equal amplitudes. The discrete version is used for time series data, and the convolution is carried out efficiently in Fourier space using fast Fourier transforms.

Figure 6 shows a contour plot of the magnitude of the wavelet coefficients for the first 4096 records of the data produced by a forcing level of 0.3. The signal energy lies mainly in the range $0.07 < \omega_\delta < 0.15$ with a

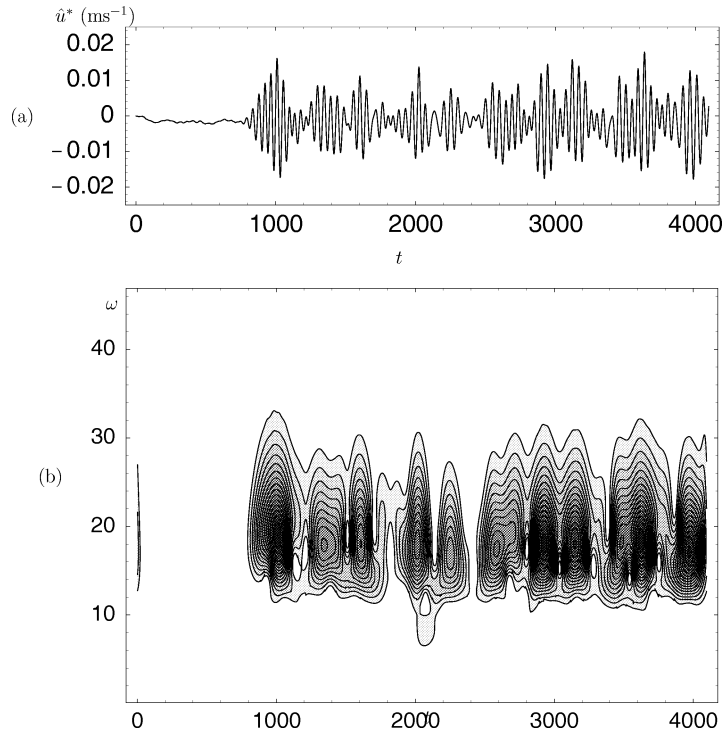

Figure 7. Same as *figure 6*, but with a forcing of 0.35.

maximum near $\omega_\delta = 0.1$. This corresponds to the band of most amplified Tollmien–Schlicting waves at this Reynolds numbers (but not the most unstable waves, since it is the net growth from the disturbance source to the measurement position which is important). *Figure 7* shows the wavelet plane for a forcing level of 0.35. A small localized region of subharmonic activity is found near record 2000, at a frequency of approximately half that of the waves with largest amplitude. This is just where *figure 3*(*b*) shows the strongest steepening is taking place. Furthermore, the maximum in the subharmonic band occurs just after the corresponding maximum in the carrier wave band. This shows that the subharmonic behaviour is strongest at a position where the carrier wave is decaying, rather than at the point where the carrier wave is strongest.

Figure 8 shows the magnitude of the wavelet coefficients for the data shown in *figure 7* at the frequency where the largest amplitudes occur and at half this frequency. Note that the spike will ultimately form near record 2000 despite the fact that the amplitude here, although a local maximum, is significantly smaller than that of nearby local maxima. This shows that amplitude alone is not the criteria for breakdown to spikes. The maximum in the subharmonic frequency is delayed by 62 records, or just over two periods of the carrier wave, relative to the corresponding maximum of the wavelets at the carrier wave frequency. In fact, over the whole 32768 records that were measured at this amplitude, the subharmonic activity is delayed relative to the carrier wave by 79 records, as can be seen from the correlation function, shown in *figure 9*, calculated using $|W|$ at the carrier wave frequency $\omega_\delta = 0.1$ and $|W|$ at the subharmonic frequency $\omega_\delta = 0.05$. This systematic negative delay between maxima in the carrier wave and maxima of subharmonic activity reinforces the conclusion that the subharmonic resonance is most active for decaying sections of the carrier wave.

The resonant interaction equations for waves whose frequencies and streamwise wavenumbers are in a 2:1 ratio, like Craik's resonant triad, have a quadratic nonlinearity rather than the cubic nonlinearity appearing in (1) and (4). This leads to a nonlinear evolution that depends on the relative phases between the interacting

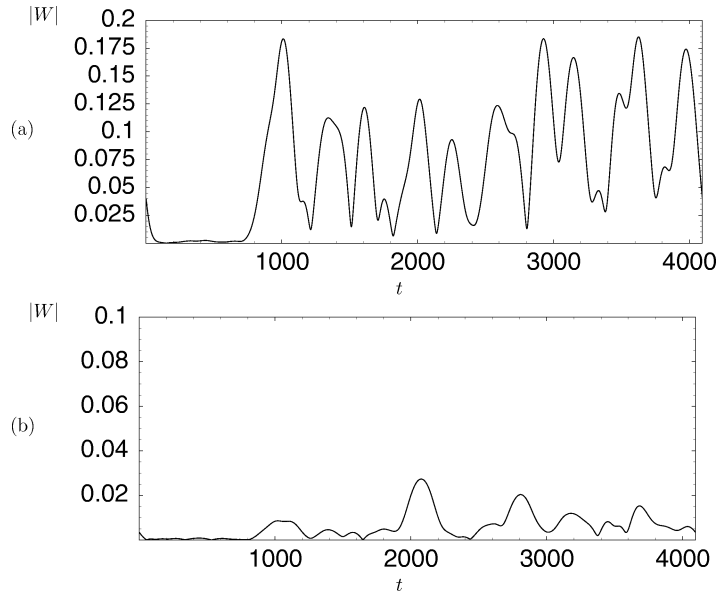

Figure 8. Magnitude of the wavelet coefficients for a forcing amplitude of 0.35 at frequencies (a) $\omega_\delta = 0.1$, (b) $\omega_\delta = 0.05$.

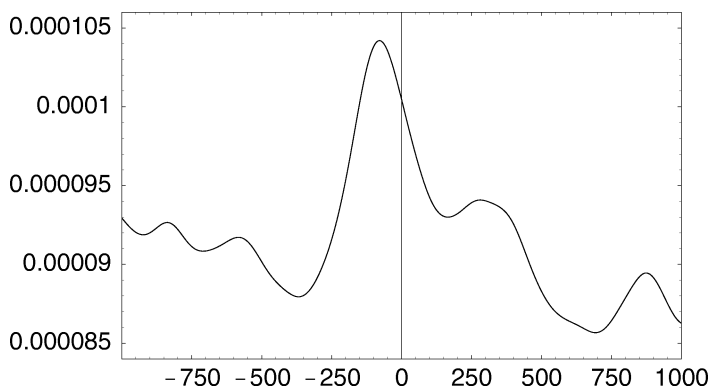

Figure 9. Graph of the correlation function against delay time for the data sets shown in *figure 7*, but calculated using all 32768 records of data measured, and not just the 4096 records shown in that figure. Negative delay times correspond to the subharmonic wave lagging behind the carrier wave frequency.

waves, as shown, for example, in section 5 of Healey [11], and which is seen in experiments on modulated waves in *figures 10* and *11* in Healey [11] and in the experiments on wavepackets by Medeiros and Gaster [10]. Here we check for phase dependence in our experiments on randomly modulated waves. *Figure 10* shows the time series data for a forcing amplitude of 0.7. There is characteristic spike behaviour near records 2000 and 23400, and the behaviour near records 16200, 28100 and 31100 corresponds to the early stages of spike development. When the forcing amplitude is increased further these latter regions develop into spikes, and more spikes emerge at other positions in the data. For large enough forcing levels, the spikes merge to give essentially turbulent behaviour.

The elements of the dynamics producing the disturbance shown in *figure 10* that depend on nonresonant evolution would be unaffected by multiplying the driving signal by -1. The elements of the dynamics that depend on resonant evolution will be affected by multiplying by -1 since this changes the signs of the coefficients of the quadratic interaction terms. *Figure 11* shows the data for a forcing signal that was -1

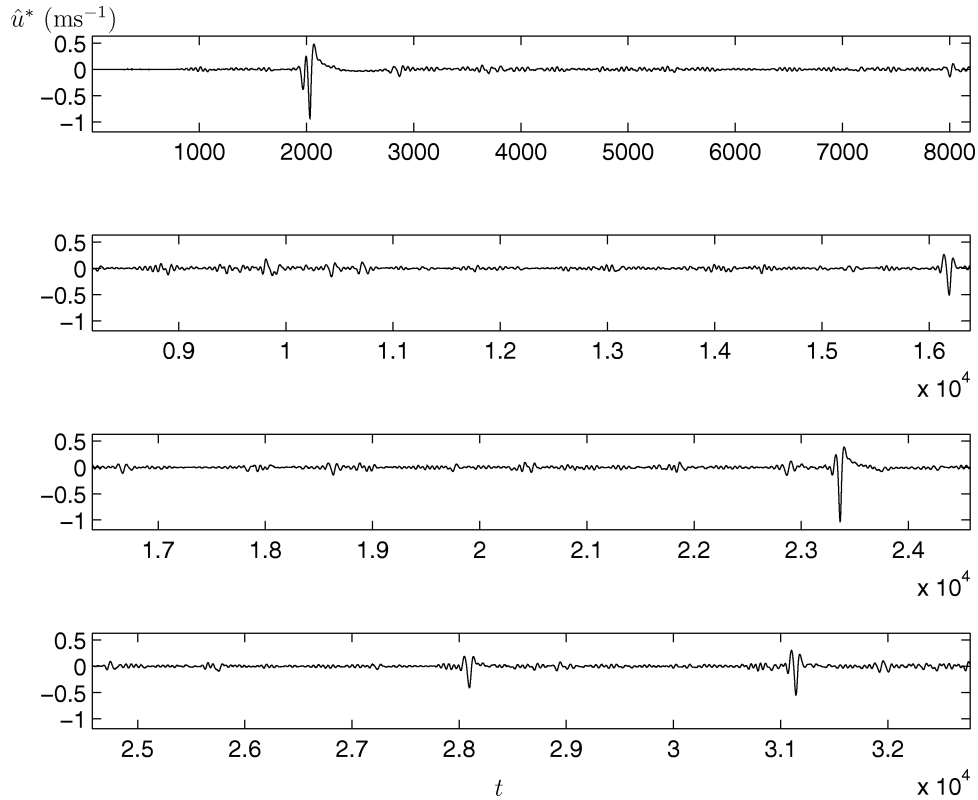

Figure 10. Hot-wire time series data (ensemble averaged) produced by a forcing amplitude of 0.7 in arbitrary units. $\hat{u}^*$ is the dimensional horizontal component of the disturbance velocity and t is the time variable in arbitrary units.

times that which produced the data shown in *figure 10*. The spikes, and incipient spikes, have moved positions, confirming that resonant interactions play an important role at some point during the evolution that leads to the spike.

6. Conclusions

The higher-order Ginzburg–Landau equation describes the weakly nonlinear evolution of modulated waves, and contains terms that produce an asymmetric envelope-steepening effect, in which either decaying or growing sections of modulation will progressively steepen, depending on the sign of certain nonlinear coefficients. It is proposed here that this model may explain the wind tunnel experiments presented in Healey [11], and summarized in *figure 1*, that show a strong asymmetry between the growing and decaying sections of a modulated disturbance. A spike appeared at the decaying section when the modulation was strong enough, but not at the growing or unmodulated sections. The model presented here does not apply to the spike itself, but to the early, weakly nonlinear, stages of evolution that lead up to the appearance of the spike.

Wind tunnel experiments on randomly modulated waves, to model transition in low-turbulence environments, have been carried out to investigate whether the proposed steepening mechanism can be observed. It is found that decaying sections do become progressively steeper compared to growing sections as the amplitude of the disturbance increases. The regions that eventually produce spikes show particularly strong steepening effects well before there are any signs of a spike emerging.

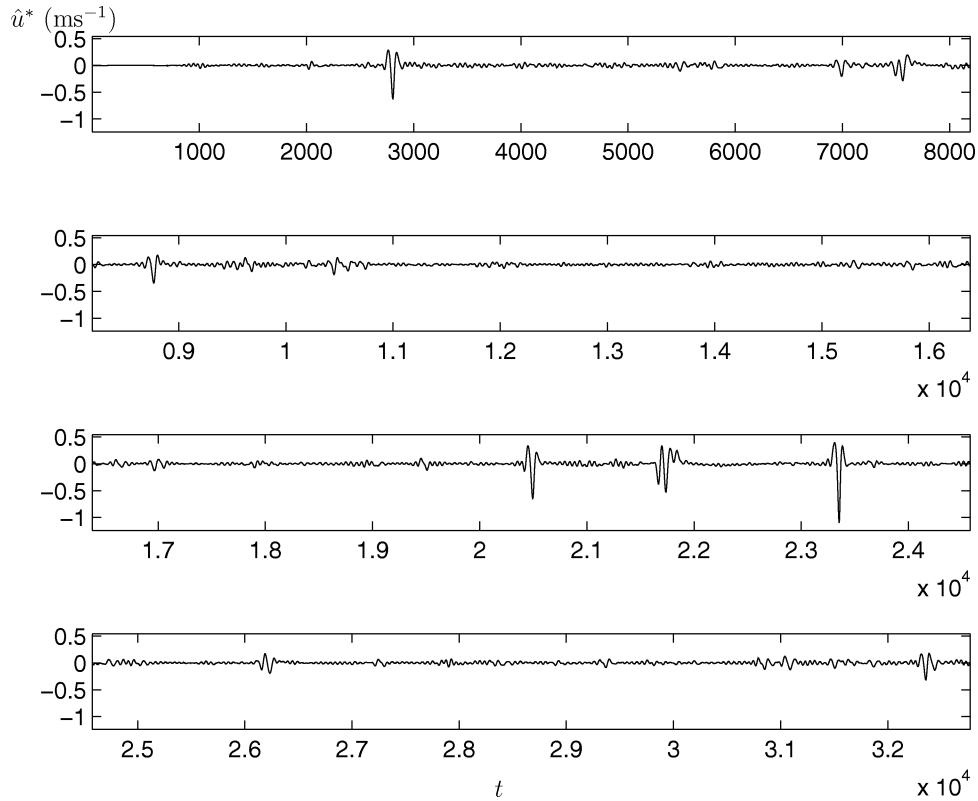

Figure 11. Hot-wire time series data (ensemble averaged) produced by a forcing amplitude of 0.7 in arbitrary units, but the forcing signal used here was -1 times the forcing signal used in *figure 10*. $\hat{u}^*$ is the dimensional horizontal component of the disturbance velocity and t is the time variable in arbitrary units.

The results of a direct numerical simulation of a two-dimensional modulated wave have also been presented. A symmetrically modulated wave similar to those shown in *figure 1* was introduced to a Blasius boundary layer, and was found to develop an asymmetry as it propagated downstream. However, this time it was the growing sections that had steepened, suggesting that the nonlinear coefficients controlling steepening for two-dimensional waves have the opposite sign to those controlling steepening for the three-dimensional waves present in the experiment. It was found that there was an increase in amplitude close to where steepening is taking place, which may be related to a focusing effect as parts of the envelope with different amplitudes coalesce. This may be a mechanism for how modulation can enhance nonlinear breakdown.

A wavelet analysis of the experimental data showed that the regions where steepening occurs are also regions where localized subharmonic activity is taking place. The subharmonic behaviour is consistent with Craik's resonant triad interaction, which involves three-dimensional waves, and the phase-dependence expected from amplitude equations with quadratic interactions was found in the experiment. A resonant equation for modulated interacting two- and three-dimensional waves can also be written down and the steepening terms may well have different coefficients than those of the two-dimensional waves studied in the direct numerical simulations. Resonant interaction takes place at lower amplitudes than required for nonresonant evolution. Therefore, it may be that the experiments are dominated by resonant interaction with three-dimensional waves; a mechanism that is absent in the two-dimensional simulation.

A curious observation made by Medeiros and Gaster [10] was that if the subharmonic part of the disturbance spectrum is removed from the driving signal, it was found to be rapidly replaced as the disturbance propagated downstream. If the subharmonic contribution to the resonant interaction is being fed by random background disturbances uncorrelated to the driving signal, then this behaviour would not be reproducible from one run of the experiment to the next. However, they observed a high degree of reproducibility. It may be that the Eckhaus instability mechanism for modulated waves is particularly strong for the Blasius boundary layer due to the small value of l_r in (14), and that this quickly amplifies the subharmonic components. If these components then reach a saturated nonlinear state, they will be essentially independent of their initial conditions, thus explaining the high degree of reproducibility in the ensueing subharmonic resonant interactions. The amplification of modulated disturbances can then feed the steepening process.

Whatever the precise details of how envelope steepening leads to spikes, it is certainly noteworthy that spikes occur first at places in the data where steepening effects and subharmonic interactions also first become active. This happens during the weakly nonlinear stages of disturbance evolution, and well before the spikes themselves appear. This indicates that weakly nonlinear theories can be used to help us to understand the early stages of breakdown to spikes, which then lead to turbulent spots and eventually to turbulence.

Acknowledgements

The experiments were carried out at the low-turbulence transition windtunnel in the Department of Engineering, Cambridge University, while the author was being supported by EPSRC grant GR/H/79778 held by M. Gaster and D.G. Crighton. The author acknowledges the help in setting up the basic flow of M.A.F. Medeiros and F.N. Shaikh. The numerical simulation was carried out by S. Houten using codes developed from ones provided by C. Davies.

References

[1] Gaster M., The physical process causing breakdown to turbulence, in: 12th Naval Hydrodynamics Symposium, Washington, 1978.
[2] Stewartson K., Stuart J.T., A nonlinear instability theory for a wave system in plane Poiseuille flow, J. Fluid Mech. 48 (1971) 529–545.
[3] Eckhaus W., Problèmes non linéaires de stabilité dans un espace a deux dimensions. Deuxième partie: stabilité des solutions périodiques, J. Méc. 2 (1963) 153–172.
[4] Eckhaus W., Studies in Nonlinear Stability Theory, Springer, Berlin, 1965.
[5] Eckhaus W., Iooss G., Strong selection or rejection of spatially periodic patterns in degenerate bifurcations, Physica D 39 (1989) 124–146.
[6] Shaikh F.N., Gaster M., The nonlinear evolution of modulated waves in a boundary layer, J. Engng. Maths. 28 (1994) 55–71.
[7] Shaikh F.N., Investigation of transition to turbulence using white-noise excitation and local analysis techniques, J. Fluid Mech. 348 (1997) 29–83.
[8] Shaikh F.N., The generation of turbulent spots in a laminar boundary layer, Eur. J. Mech. B/Fluids 16 (1997) 349–385.
[9] Medeiros M.A.F., Gaster M., The influence of phase on the nonlinear evolution of wavepackets in boundary layers, J. Fluid Mech. 397 (1999) 259–283.
[10] Medeiros M.A.F., Gaster M., The production of subharmonic waves in the nonlinear evolution of wavepackets in boundary layers, J. Fluid Mech. 399 (1999) 301–318.
[11] Healey J.J., A new boundary-layer resonance enhanced by wave modulation: theory and experiment, J. Fluid Mech. 304 (1995) 231–262.
[12] Amini J., Lespinard G., Experimental study of an ‘incipient spot’ in a transitional boundary layer, Phys. Fluids 25 (1982) 1743–1750.
[13] Klingmann B.G.B., On transition due to three-dimensional disturbances in plane Poiseuille flow, J. Fluid Mech. 240 (1992) 167–195.
[14] Stuart J.T., On the non-linear mechanics of wave disturbances in stable and unstable parallel flows. Part 1. The basic behaviour of plane Poiseuille flow, J. Fluid Mech. 9 (1960) 353–370.
[15] Watson J., On spatially-growing finite disturbances in plane Poiseuille flow, J. Fluid Mech. 14 (1962) 211–221.
[16] Fasel H., Konzelmann U., Nonparallel stability of a flat-plate boundary-layer using the complete Navier–Stokes equations, J. Fluid Mech. 221 (1990) 311–347.
[17] Bertolotti F.P., Herbert T., Spalart P.R., Linear and nonlinear stability of the Blasius boundary-layer, J. Fluid Mech. 242 (1992) 441–474.
[18] Klingmann B.G.B., Boiko A.V., Westin K.J.A., Kozlov V.V., Alfredsson P.H., Experiments on the stability of Tollmien–Schlicting waves, Eur. J. Mech. B/Fluids 12 (1993) 493–514.

[19] Ruban A.I., Nonlinear equation for the amplitude of the Tollmien–Schlichting waves in the boundary layer, Izv. Akad. Nauk SSSR, Mech. Zhidk. & Gaza 6 (1983) 60–67.
[20] Hall P., Smith F.T., On the effects of nonparallelism, three-dimensionality, and mode interaction in nonlinear boundary layer stability, Stud. Appl. Math. 70 (1984) 91–120.
[21] Smith F.T., Nonlinear stability of boundary layers for disturbances of various sizes, P. Roy. Soc. Lond. A Mat. 368 (1979) 573–589.
[22] Smith F.T., Corrections to 'Nonlinear stability of boundary layers for disturbances of various sizes', P. Roy. Soc. Lond. A Mat. 371 (1980) 439–440.
[23] Hultgren L.S., Higher eigenmodes in the Blasius boundary layer stability problem, Phys. Fluids 30 (1987) 2947–2951.
[24] Healey J.J., On why oblique waves in the Blasius boundary layer show stronger nonparallel effects than planar waves, in: Fasel H., Saric W.S. (Eds), P. IUTAM Symp. Laminar-Turbulent Transition, Sedona, Arizona, USA, Sept. 1999, Springer-Verlag, 2000.
[25] Healey J.J., Characterizing boundary-layer instability at finite Reynolds numbers, Eur. J. Mech. B/Fluids 17 (1998) 219–237.
[26] Healey J.J., On the neutral curve of the flat-plate boundary-layer: comparison between experiment, Orr–Sommerfeld theory and asymptotic theory, J. Fluid Mech. 288 (1995) 59–73.
[27] Benjamin T.B., The development of three-dimensional disturbances in an unstable film of liquid flowing down an inclined plane, J. Fluid Mech. 10 (1961) 401–419.
[28] Jennings M.J., Stewart P.A., Cowley S.J., When is the weakly nonlinear evolution of a localized disturbance governed by the Ginzburg–Landau equation?, P. Roy. Soc. Lond. A Mat. 455 (1999) 1521–1560.
[29] Stuart J.T., DiPrima R.C., The Eckhaus and Benjamin–Feir resonance mechanisms, P. Roy. Soc. Lond. A Mat. 362 (1978) 27–41.
[30] Benjamin T.B., Feir J.E., The disintegration of wave trains on deep water, J. Fluid Mech. 27 (1967) 417–430.
[31] Ikeda M., Nonlinearity and nonperiodicity of a two-dimensional disturbance in plane Poiseuille flow, J. Phys. Soc. Jpn 42 (1977) 1764–1771.
[32] Weinstein M., Nonlinear instability in plane Poiseuille flow: a quantitative comparison between the methods of amplitude expansions and the method of multiple scales, P. Roy. Soc. Lond. A Mat. 375 (1981) 155–167.
[33] Johnson R.S., On the modulation of water waves in the neighbourhood of $kh \approx 1.363$, P. Roy. Soc. Lond. A Mat. 357 (1977) 131–141.
[34] Dysthe K.B., Note on a modification to the nonlinear Schrödinger equation for application to deep water waves, P. Roy. Soc. Lond. A Mat. 369 (1979) 105–114.
[35] Sen P.K., Vashist T.K., On the nonlinear stability of boundary-layer flow over a flat plate, P. Roy. Soc. Lond. A Mat. 424 (1989) 81–92.
[36] Houten S., Healey J.J., Davies C., Nonlinear evolution of Tollmien–Schlichting waves at finite Reynolds numbers, in: Fasel H., Saric W.S. (Eds), P. IUTAM Symp. Laminar-Turbulent Transition, Sedona, Arizona, USA, Sept. 1999, Springer-Verlag, 2000.
[37] Houten S., Healey J.J., Davies C., Direct numerical simulations of modulated and unmodulated nonlinear waves in the Blasius boundary layer, J. Fluid Mech. (2001) (In preparation).
[38] Moresco P., Healey J.J., Weakly nonlinear stability analysis of a family of mixed convection boundary layers, J. Fluid Mech. (2001) (In preparation).
[39] Li L., Walker J.D.A., Bowles R.I., Smith F.T., Short-scale break-up in unsteady interactive layers: local development of normal pressure gradients and vortex wind-up, J. Fluid Mech. 374 (1998) 335–378.
[40] Gaster M., Grant I., An experimental investigation into the formation and development of a wave packet in a laminar boundary layer, P. Roy. Soc. Lond. A Mat. 347 (1975) 253–269.
[41] Gaster M., The nonlinear phase of wave growth leading to chaos and breakdown to turbulence in a boundary layer as an example of an open system, P. Roy. Soc. Lond. A Mat. 430 (1990) 3–24.
[42] Davies C., Carpenter P.W., Numerical simulation of the evolution of Tollmien–Schlichting waves over finite compliant panels, J. Fluid Mech. 335 (1997) 361–392.
[43] Craik A.D.D., Nonlinear resonant instability in boundary layers, J. Fluid Mech. 50 (1971) 393–413.